

File ID uvapub:1859
Filename 20442y.pdf
Version unknown

SOURCE (OR PART OF THE FOLLOWING SOURCE):

Type article
Title The ISO-SWS spectrum of NML Cygni
Author(s) K. Justtanont, T. de Jong, F.P. Helmich, L.B.F.M. Waters, Th. de Graauw, C.
 Loup, H. Izumiura, I. Yamamura, D.A. Beintema, F. Lahuis, P.R. Roelfsema,
 E.A. Valentijn
Faculty FNWI: Astronomical Institute Anton Pannekoek (IAP)
Year 1996

FULL BIBLIOGRAPHIC DETAILS:

<http://hdl.handle.net/11245/1.127107>

Copyright

It is not permitted to download or to forward/distribute the text or part of it without the consent of the author(s) and/or copyright holder(s), other than for strictly personal, individual use, unless the work is under an open content licence (like Creative Commons).

The ISO-SWS spectrum of NML Cyg[★]

K. Justtanont¹, T. de Jong^{1,2}, F.P. Helmich³, L.B.F.M. Waters^{2,1}, Th. de Graauw¹, C. Loup⁴, H. Izumiura⁵, I. Yamamura^{6,1}, D.A. Beintema¹, F. Lahuis^{1,7}, P.R. Roelfsema¹, and E.A. Valentijn¹

¹ SRON/Groningen, P.O.Box 800, 9700 AV Groningen, The Netherlands

² Astronomical Institute ‘Anton Pannekoek’, University of Amsterdam, Kruislaan 403, 1098 SJ Amsterdam, The Netherlands

³ Leiden Observatory, P.O. Box 9513, 2300 RA Leiden, The Netherlands

⁴ Institut d’Astrophysique, 98 bis Bd Arago, F-75014 Paris, France

⁵ Okayama Astrophysical Observatory, National Astronomical Observatory, Kamogata, Asaguchi, Okayama 719-02, Japan

⁶ Department of Astronomy, University of Tokyo, 2-11-16 Yayoi-cho, Bunkyo-ku, Tokyo 113, Japan

⁷ SIDT, ESA Villafranca, P.O. Box 50727, E-28080 Madrid, Spain

Received 16 July 1996 / Accepted 2 August 1996

Abstract. The high resolution spectrum of NML Cyg observed with the ISO-SWS in its slow-speed grating mode (2.4–45 μm) shows a wealth of features never seen before in previous observations. These include ro-vibrational lines of H₂O at 2.7 and 6.2 μm , of OH between 3 and 3.5 μm and a deep absorption band of CO₂ at 4.26 μm . We also report on the detection of pure rotational emission lines of H₂O between 35 and 45 μm and of the 34.6 μm absorption line of OH which is thought to pump the well known 1612 MHz OH maser line. There are two, as yet, unidentified features at 33 and 40 μm which may be related to silicate dust.

Key words: stars: AGB and post-AGB – stars: circumstellar matter – stars: individual (NML Cyg) – stars: late-type – infrared: stars

27.7 km s⁻¹ and an OH shell radius of 3 arcseconds (corresponding to 8×10^{16} cm at 1.8 kpc). NML Cyg also exhibits SiO maser emission (Snyder & Buhl 1975) and H₂O maser emission (Engels, Schmid-Burgk, & Walmsley 1988). The SiO maser lines show strong variability on a timescale of a few days probably related to stellar activity since SiO masers are thought to originate very close to the star, within the dust condensation radius. The central star is rendered invisible by the large dust column density in the circumstellar shell, resulting in a silicate absorption at 9.7 μm . Nercessian et al. (1989) have reported the detection of CO J=1-0 and HCN J=1-0. The radius of the inner dust shell was measured in the near-IR by Ridgway et al. (1986) and Benson, Turner & Dyck (1989) to be 0''.05 (corresponding to about 10^{15} cm at 1.8 kpc).

NML Cyg is one of the prime objects in the guaranteed time proposal to study bright AGB stars and cool supergiants (PI T. de Jong) with the Short Wavelength Spectrometer (SWS) on board ISO (Kessler et al. 1996), as part of the observing program of the SWS consortium.

In this letter, we present and discuss the full 2–45 μm SWS grating spectrum of NML Cyg. In Sect. 2 we briefly describe the observation and in Sect. 3 we discuss the main molecular features detected in the SWS spectrum.

2. Observation

The observation was carried out with the SWS during the performance verification phase on 8 January 1996 with the slowest full grating scan speed (AOT 1, speed 4), achieving a spectral resolution ranging from 1400 at 2.3 μm to 680 at 30 μm .

NML Cyg is a point source for the SWS beam. The data were reduced using the standard SWS data reduction software package provided by the SWS Instrument Dedicated Team. The present reduction should be considered preliminary because fine-tuning is still going on. Although flux levels may be af-

1. Introduction

NML Cyg is one of the brightest sources in the northern sky at near-infrared wavelengths. It was discovered by Neugebauer, Martz & Leighton (1965) during the all-sky survey that eventually resulted in the InfraRed Catalog (IRC). Later studies have shown that it is a cool supergiant (spectral type M6, luminosity $\sim 5 \times 10^5 L_{\odot}$) experiencing strong mass loss ($\sim 2 \times 10^{-4} M_{\odot} \text{yr}^{-1}$) and surrounded by a very thick circumstellar shell at a distance of about 1.8 kpc (Bowers, Johnson & Spencer 1983; Ridgway et al. 1986). From its very strong OH maser emission Bowers et al. (1983) determined an OH expansion velocity of

[★] Based on observations with ISO, an ESA project with instruments funded by ESA Member States (especially the PI countries: France, Germany, the Netherlands and the United Kingdom) and with the participation of ISAS and NASA

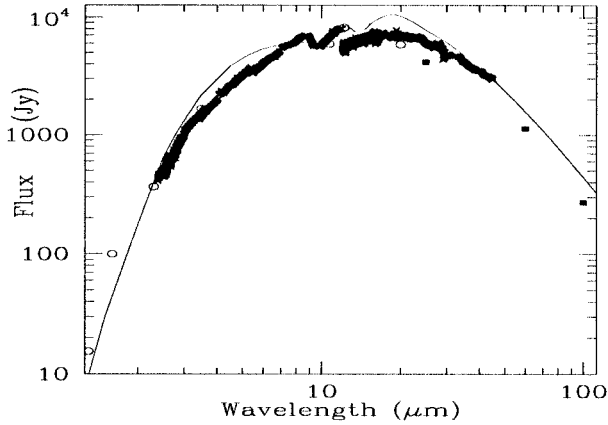


Fig. 1. The spectral energy distribution of NML Cyg. Open circles represent ground-based photometry and solid squares are from the IRAS PSC. Crosses represent the SWS data adjusted to match the ground-based photometry (estimated absolute flux uncertainty 30%) and the curve represents our model fit.

ected by the uncertainty in the dark current measured during the observation, the high flux levels ensure that this effect is minimal. The main uncertainty in the observed flux comes from the pointing uncertainty and the relative spectral response function (RSRF). The estimated uncertainty in the flux level is of the order of 30% (see de Graauw et al. 1996, this volume for more details of the instrument and observing procedures).

3. Discussion

Using the model of Justtanont & Tielens (1992) we have attempted to fit the observed SWS spectrum supplemented with near-infrared photometry data of Strecker & Ney (1974) and IRAS data at long wavelengths (Fig. 1). Adopting a distance of 1.8 kpc and assuming spherical symmetry in the shell and a constant outflow velocity of 27.7 km s^{-1} , we obtain a dust mass loss rate of $2 \times 10^{-6} M_{\odot} \text{ yr}^{-1}$, in good agreement with the observed mass loss rate of $2 \times 10^{-4} M_{\odot} \text{ yr}^{-1}$ for a nominal value of the gas-to-dust mass ratio of 100. The calculated infrared luminosity equals $5 \times 10^5 L_{\odot}$ with the inner radius of the shell placed at $9 R_{*}$, where $R_{*} = 1.8 \times 10^{14} \text{ cm}$. These values are consistent with the speckle results by Ridgway et al. (1986). The calculated optical depth of the $9.7 \mu\text{m}$ silicate feature in our model is 4.4. Note that there is a large discrepancy between ground-based photometry, IRAS photometry and the SWS spectrum between $12\text{--}25 \mu\text{m}$. We have assumed a dust FIR efficiency fall off as $\lambda^{-1.5}$.

Several molecular absorption features show up very prominently in the spectrum of NML Cyg. First we discuss the fundamental ro-vibrational band of CO at $4.6 \mu\text{m}$ which is resolved into individual lines spanning 4.5 to $4.9 \mu\text{m}$ (Fig. 2). For both the P- and R-branches, we can see lines up to $J=24$. In order to study the band in more detail we have divided out the continuum. To do so, we determined the local continuum in the observed spectrum by fitting straight lines to it.

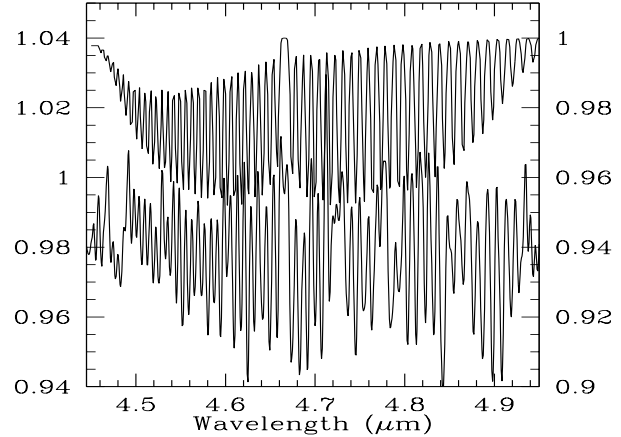


Fig. 2. The continuum divided spectrum showing CO absorption (bottom) and the modelled spectrum with $T_{\text{ex}} = 300\text{K}$, $b_{\text{D}} = 3 \text{ km s}^{-1}$ and $N = 10^{19} \text{ cm}^{-2}$.

In an attempt to derive molecular column densities and excitation temperatures from the observations we have modelled the absorption lines assuming thermodynamic equilibrium using the computer code and molecular data for CO provided by Helmich (1996 and references therein). The required input parameters for this model are the column density, N , the Doppler parameter, b_{D} and the excitation temperature, T_{ex} . For the best fit of this band we estimate an excitation temperature of 300 K from the extent of the band and the presence of the highest rotational lines. The SWS resolution is sufficiently high to detect individual ro-vibrational lines but is too coarse to resolve them. Hence, we have to assume a line width in order to model the spectrum. For $b_{\text{D}} = 3 \text{ km s}^{-1}$, we find a “best fit” for $N = 10^{19} \text{ cm}^{-2}$ (Fig. 2). The modelled spectrum has been rebinned to the SWS resolution for comparison with the observed spectrum. The observations constrain the estimated kinetic gas temperature rather well but the column density is uncertain by at least a factor of two. We cannot confirm any detection of ^{13}CO in our spectrum indicating that $^{13}\text{CO}/^{12}\text{CO}$ is less than 0.1. Although CO is thought to form in the photosphere, the low excitation temperature suggests that the band comes from farther out in the circumstellar envelope due to the large dust optical depth at this wavelength.

Since observations with ISO from space do not suffer from atmospheric absorption we are able to report here the first detection of H_2O in the spectrum of NML Cyg. In the SWS wavelength range, we see both pure rotational and ro-vibrational lines of gas phase H_2O . For the ν_2 ro-vibrational band at $6.2 \mu\text{m}$ (bending mode), we estimate the column density in a similar manner as for CO (Fig. 3). The molecular data have been taken from Camy-Peyret & Flaud (1976), Crovisier (1992) and Hitran (Rothman et al. 1987) From the lack of high ro-vibrational lines towards the edge of the band, the excitation temperature for this band is relatively low compared to CO. We estimate the excitation temperature to be only 100 K. Assuming $b_{\text{D}} = 2.0 \text{ km s}^{-1}$, we find the best fit for a column density of 2×10^{19}

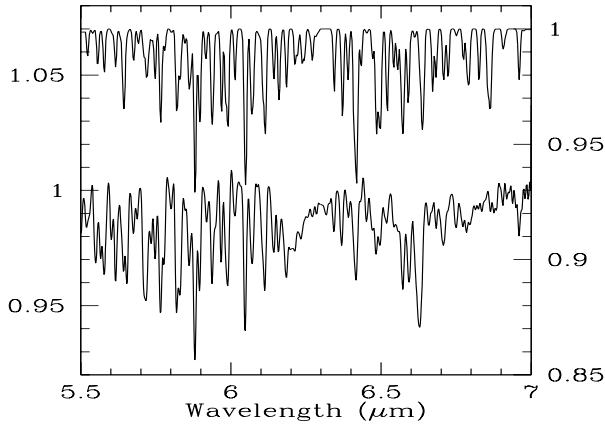


Fig. 3. The continuum divided spectrum showing the ν_2 band of H_2O in absorption (bottom) and the modelled spectrum with $T_{\text{ex}} = 100\text{K}$, $b_{\text{D}} = 2 \text{ km s}^{-1}$ and $N = \times 10^{19} \text{ cm}^{-2}$.

cm^{-2} . Again, the column density is not as well constrained as the temperature and may easily be uncertain by a factor 2.

There is also another H_2O ro-vibrational band observed at $2.7 \mu\text{m}$. This is a blend of the ν_1 and ν_3 stretching bands. We have modelled this using the above model in order to derive the gas temperature and column density. For the ν_3 band, we assume the same line width and column density as for the $6.2 \mu\text{m}$ band. The excitation temperature for this band is assumed to be about 500 K . We are not, however, able to fit the observed spectrum because at this temperature, we do not excite the higher transition lines seen in the observed spectrum. At present, we do not have molecular data for $T > 500 \text{ K}$. From this, we conclude that this band must come from a hot region interior to where the $6.2 \mu\text{m}$ band is formed, possibly probing the acceleration zone of the outflow. We also calculated the contribution from the ν_1 band but the absorption lines from this band are weaker than in the ν_3 band. The fit is as poor as for the ν_3 band so that no firm conclusions can be drawn.

The spectrum of NML Cyg also shows a series of absorption bands between $3 - 3.5 \mu\text{m}$ which we attribute to OH absorption. We have confirmed this by comparing wavelengths of absorption features with those from the Hitran database (Rothman et al. 1987) Ro-vibrational lines in the fundamental bands ($v = 0, {}^2\Pi_{3/2}$ to $v = 1, {}^2\Pi_{3/2}$ and $v = 0, {}^2\Pi_{1/2}$ to $v = 1, {}^2\Pi_{1/2}$) of OH observed in the spectrum of NML Cyg are shown in Fig. 4.

We have also detected for the first time the $4.2 \mu\text{m}$ CO_2 absorption band in NML Cyg (Fig. 5). CO_2 can be formed in the warm circumstellar environment via reactions between CO and OH (Nercessian et al. 1989) because this reaction has an activation barrier of about 80K . We do not resolve the band into individual lines as seen in the gas phase CO. Our model fit requires $T_{\text{ex}} = 250 \text{ K}$, $b_{\text{D}} = 2 \text{ km s}^{-1}$ and $N = 2 \times 10^{18} \text{ cm}^{-2}$. The width of the observed spectrum suggests the presence of ${}^{13}\text{CO}_2$ with an upper limit to the column density of $2 \times 10^{16} \text{ cm}^{-2}$. Note that the residual spectrum after fitting CO_2 has a regular pattern

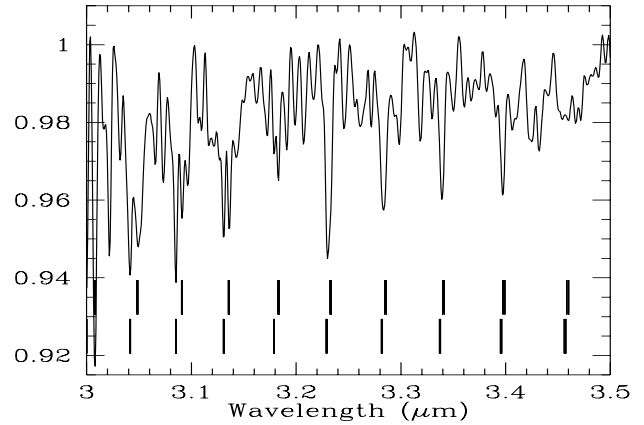


Fig. 4. The continuum divided spectrum showing the OH absorption band. Vertical lines are positions of lines in the $v = 0 {}^2\Pi_{3/2}$ to $v = 1 {}^2\Pi_{3/2}$ (the upper set) and $v = 0 {}^2\Pi_{1/2}$ to $v = 1, {}^2\Pi_{1/2}$ ro-vibrational bands.

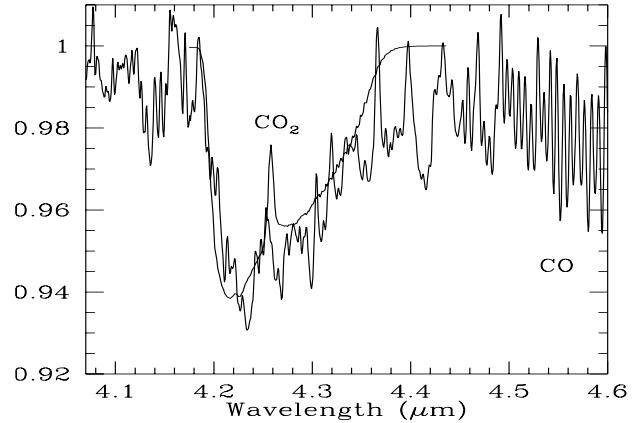


Fig. 5. The continuum divided spectrum showing the CO_2 band. The parameters for the fit are $T_{\text{ex}} = 250 \text{ K}$, $b_{\text{D}} = 2 \text{ km s}^{-1}$ and $N = 2 \times 10^{18} \text{ cm}^{-2}$ for ${}^{12}\text{CO}_2$.

of absorption which has yet to be identified. We do not detect the $15.2 \mu\text{m}$ bending mode of CO_2 . This is not surprising since it has a much smaller band strength compared to the stretching mode at $4.2 \mu\text{m}$ and also the strong effect of fringing in the data due to the problematic RSRF.

A very important absorption line that we report here is the OH absorption at $34.6 \mu\text{m}$ (${}^2\Pi_{3/2} J=3/2$ to ${}^2\Pi_{1/2} J=5/2$) which is thought to be responsible for pumping the OH maser 1612 MHz satellite line (Elitzur, Goldreich & Scoville 1976) widely observed in AGB stars. Unfortunately, the resolution of our grating scan is not high enough to resolve the OH doublet structure. Herman et al. (1986) showed a good correlation between the 35 and $53 \mu\text{m}$ luminosity and the OH maser luminosity for OH/IR stars and they confirmed the theoretical pump efficiency of 25% . From the FWHM of the line, we derive a lower limit to the OH column density of $\sim 10^{17} \text{ cm}^{-2}$, consistent with the observed mass loss rate of $2 \times 10^{-4} M_{\odot} \text{ yr}^{-1}$ and an OH abundance $\gtrsim 7 \times 10^{-5}$ in a masing shell located at $8 \times 10^{16} \text{ cm}$.

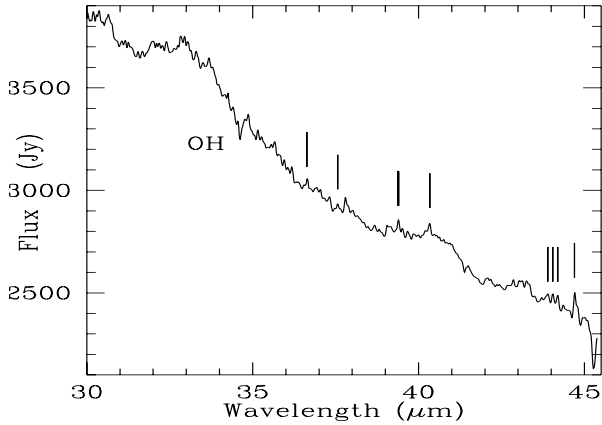


Fig. 6. The spectrum in the long wavelength band of NML Cyg. Vertical lines mark positions of preliminary detection of rotational water lines.

Table 1. The list of preliminary detected H₂O rotational lines. o=ortho-H₂O; p=para-H₂O

Transition	$\lambda(\mu\text{m})$	Transition	$\lambda(\mu\text{m})$
8 ₅₃ – 8 ₂₆	36.64	p 5 ₄₁ – 4 ₃₂	43.89
7 ₄₄ – 6 ₃₃	37.57	p 7 ₄₃ – 7 ₁₆	44.05
5 ₅₀ – 4 ₄₁	39.37	o 5 ₄₂ – 4 ₃₁	44.19
5 ₅₁ – 4 ₄₀	39.38	p 8 ₃₆ – 7 ₂₅	44.70
6 ₄₃ – 5 ₃₂	40.34	o	

The long wavelength part of the SWS spectrum shows a number of narrow emission lines between 30 and 45 μm . Given that the RSRF is relatively featureless in this region, we expect that many of these lines are real. Here, we present preliminary identifications of a number of highly excited pure rotational H₂O lines in the spectrum of NML Cyg. The ones that we have identified are indicated in Fig. 6 and listed in Table 1. They appear in both the up and down scans of the spectrum and, eventhough formally only detected at the 2σ level, are probably real. All lines require an excitation temperature $\gtrsim 500$ K therefore they must originate close to the central star. Detection of these rotational lines is very important since H₂O is very efficient in cooling the gas in the circumstellar envelope by radiative cooling (Goldreich & Scoville 1976; Chen & Neufeld 1995).

Finally, we observe two broad features between 31.5–36 μm and 39–42 μm . These features are not artifacts of the data reduction and are also seen in the SWS spectrum of O-rich post-AGB stars and planetary nebulae (Waters et al. 1996, this volume). The width of both features suggests that they arise from solid state material rather than that they are of molecular origin. They may be due to silicate-type dust or other O-rich dust. Waters et al. propose that the existence of these features indicates that some fraction of the silicate in these envelopes is crystalline. This may mean that dust is formed at higher temperatures than commonly adopted for amorphous grains, i.e. closer to the central star.

Acknowledgements. We wish to thank the SIDT for support and suggestions on data reduction and for their hospitality during our trips to Vilsba.

References

- Benson, J.A., Turner, N.H., Dyck, H.M., 1989, *AJ*, 97, 1763
 Bowers, P.F., Johnson, K.J., Spencer, J.H., 1983, *ApJ*, 274, 733
 Camy-Peyret, C., Flaud, J.-M., 1976, *Molec. Phys.*, 32, 523
 Chen, W., Neufeld, D.A., 1995, *ApJ*, 453, L99
 Crovisier, J., 1992, in *Constants for Molecules of Astrophysical Interest in the Gas-phase*, Obs. de Meudon
 de Graauw, Th., et al., 1996, *A&A*, this volume
 Elitzur, M., Goldreich, P., Scoville, N., 1976, *ApJ*, 205, 384
 Engels, D., Schmid-Burgk, J., Walmsley, C.M., 1988, *A&A*, 191, 283
 Goldreich, P., Scoville, N., 1976, *ApJ*, 205, 144
 Herman, J., Burger, J.H., Penninx, W.H., 1986, *A&A*, 167, 247
 Helmich, F.P., 1996, PhD thesis (Leiden)
 Justtanont, K., Tielens, A.G.G.M., 1992, *ApJ*, 389, 400
 Kessler, M.F., et al., 1996, this volume
 Nercessian, E., Guilloteau, S., Omont, A., Nenayoun, J.J., 1989, *A&A*, 210, 225
 Neugebauer, G., Martz, D.E., Leighton, R.B., 1965, *ApJ*, 142, 399
 Ridgway, S.T., Joyce, R.R., Connors, D., Pipher, J.L., Dainty, C., 1986, *ApJ*, 302, 662
 Rothman, L.S., Gamache, R.R., Goldman, A., Brown, L.R., Toth, R.A., Pickett, H.M., Poynter, R.L., Flaud, J.-M., Camy-Peyret, C., Barbe, A., Husson, N., Rinsland, C.P., Smith, M.A.H., 1987, *App. Optics*, 26, 4058
 Snyder, L.E., Buhl, D., 1975, *ApJ*, 197, 340
 Strecker, D.W., Ney, E.P., 1974, *AJ*, 79, 1410
 Waters, L.B.F.M., et al., 1996, *A&A*, this volume